Brain Imaging and Behavior (2018) 12:518–531
DOI 10.1007/s11682-017-9713-z

ORIGINAL RESEARCH

Treatment effect of methylphenidate on intrinsic functional brain network in medication-naïve ADHD children: A multivariate analysis

Jae Hyun Yoo[1,2] · Dohyun Kim[1,2] · Jeewook Choi[3] · Bumseok Jeong[1,2]

Published online: 17 April 2017

Abstract Methylphenidate is a first-line therapeutic option for treating attention-deficit/hyperactivity disorder (ADHD); however, elicited changes on resting-state functional networks (RSFNs) are not well understood. This study investigated the treatment effect of methylphenidate using a variety of RSFN analyses and explored the collaborative influences of treatment-relevant RSFN changes in children with ADHD. Resting-state functional magnetic resonance imaging was acquired from 20 medication-naïve ADHD children before methylphenidate treatment and twelve weeks later. Changes in large-scale functional connectivity were defined using independent component analysis with dual regression and graph theoretical analysis. The amplitude of low frequency fluctuation (ALFF) was measured to investigate local spontaneous activity alteration. Finally, significant findings were recruited to random forest regression to identify the feature subset that best explains symptom improvement. After twelve weeks of methylphenidate administration, large-scale connectivity was increased between the left fronto-parietal RSFN and the left insula cortex and the right fronto-parietal and the brainstem, while the clustering coefficient (CC) of the global network and nodes, the left fronto-parietal, cerebellum, and occipital pole-visual network, were decreased. ALFF was increased in the bilateral superior parietal cortex and decreased in the right inferior fronto-temporal area. The subset of the local and large-scale RSFN changes, including widespread ALFF changes, the CC of the global network and the cerebellum, could explain the 27.1% variance of the ADHD Rating Scale and 13.72% of the Conner's Parent Rating Scale. Our multivariate approach suggests that the neural mechanism of methylphenidate treatment could be associated with alteration of spontaneous activity in the superior parietal cortex or widespread brain regions as well as functional segregation of the large-scale intrinsic functional network.

Keywords Attention deficit-hyperactivity disorder · Methylphenidate · Functional magnetic resonance imaging · Resting state networks · Machine learning

✉ Jeewook Choi
cjwcool@catholic.ac.kr

✉ Bumseok Jeong
bs.jeong@kaist.ac.kr

[1] Computational Affective Neuroscience and Development Laboratory, Graduate School of Medical Science and Engineering, KAIST, 291 Daehak-ro, Yoosung-gu, Daejeon 34141, Republic of Korea

[2] KI for Health Science and Technology, KAIST Institute, KAIST, 291 Daehak-ro, Yoosung-gu, Daejeon 34141, Republic of Korea

[3] Department of Psychiatry, Catholic University Daejeon St. Mary's Hospital, 64 Daeheung-ro, Jung-gu, Daejeon 34943, Republic of Korea

Background

Attention-deficit/hyperactivity disorder (ADHD) is a common neurodevelopmental disorder that affects 3 to 10% of school-aged children (Schubiner and Katragadda 2008). The symptoms in affected children include inattention, hyperactivity, and impulsivity, which are often exhibited as inappropriate

behavior, noncompliance, and negative social behavior (DuPaul et al. 2001). A multidisciplinary strategy is suggested for improving ADHD symptoms, but psychostimulant treatment, including methylphenidate (MPH), has remained a first-line therapeutic option for ADHD (Subcommittee on Attention-Deficit/Hyperactivity et al. 2011; Van der Oord et al. 2008).

The proposed mechanism of action of MPH is that it blocks both dopamine and norepinephrine transporters in the prefrontal cortex and the striatum preferentially (Berridge et al. 2006; Volkow et al. 2002). Previous functional MRI (fMRI) studies supported evidence that MPH could upregulate the activation of fronto-striatal regions in the ADHD group when tasks were being performed (Czerniak et al. 2013; Epstein et al. 2007; Konrad et al. 2007; Rubia et al. 2009). In addition, MPH-elicited changes were also consistently reported in the cerebellar regions, which showed significant increase in activity and metabolism (Czerniak et al. 2013; Epstein et al. 2007; Rubia et al. 2011; Volkow et al. 1997). Those results suggested that functional impairment in prefrontal-striatal-cerebellar circuits may play a crucial role in ADHD pathophysiology.

Recently, a growing body of evidence also pointed out that ADHD subjects also have impaired intrinsic functional architecture, including disrupted large-scale resting network organization as well as local spontaneous activity and connectivity (An et al. 2013a; Castellanos and Aoki 2016; Castellanos and Proal 2012; Fair et al. 2012; Zang et al. 2007). Although significant alterations were found across extensive brain regions, MPH effects on the resting-state functional network (RSFN) and correlated clinical improvement have been less investigated. In a previous study, MPH elicited local connectivity alteration in widespread frontal, parietal and cerebellar regions, but only a cluster in the superior parietal area showed a correlation with symptom improvement (An et al. 2013b). Another recent study revealed single-dose MPH induced decreased within-RSFN connectivity in the visual and cerebellar network as well as reduced visual network connectivity to executive and default mode networks (Silk et al. 2016). Those RSFN changes might have a mediating role in clinical improvement, but their contribution has not yet been fully discovered.

There are a number of methods for characterizing the architecture of the RSFN, including both local and large-scale approaches. For large-scale changes, a number of analytical approaches have been introduced, such as Independent Component Analysis (ICA) with dual regression (Beckmann and Smith 2004) and graph theoretical analysis (Bullmore and Sporns 2009). Furthermore, local spontaneous regional activity was estimated by data-driven approaches, including amplitude of low frequency fluctuation (ALFF) and fractional ALFF (fALFF) (Zang et al. 2007; Zou et al. 2008). Each approach has different foci of interest; thus, they can represent multi-faceted aspects of MPH treatment. We hypothesized that subsequent methods, ICA with dual regression, graph theoretical analysis, ALFF and fALFF, would capture various aspects of the intrinsic functional recovery of the ADHD subject. In addition, the findings from local and large-scale analyses could have a collaborative role in behavioral or clinical improvement with various levels of contribution.

In sum, our specific aim was to explore the significant changes in both local and large-scale RSFNs derived by short-term MPH treatment and association between RSFN change and improvement in clinical manifestation. To clarify the MPH-driven effect, we recruited ADHD subjects without prior exposure to any psychotropic medication and acquired resting-state functional magnetic resonance imaging (R-fMRI) before methylphenidate treatment and twelve weeks later. Paired analyses within the ADHD group were conducted to investigate the main effects of MPH using a variety of methods, including ICA with dual regression, graph theoretical analysis, and ALFF/fALFF. We also contrasted the RSFN changes with age-matched typically developing children (TDC). Finally, we adopted an ensemble learning algorithm called 'random forest' to determine the collaborative contribution of neuroimaging findings to symptom improvement.

Methods

Participants

Forty-three children with medication-naïve ADHD, aged 7 to 16 years old, and 28 age-matched TDC subjects were recruited by advertisements at the child and adolescent psychiatric clinic in Daejeon's St. Mary's Hospital. The Diagnostic and Statistical Manual of Mental Disorders - Fourth Edition (DSM-IV) criteria based on structured diagnostic interviews (Kiddie-Schedule for Affective Disorders and Schizophrenia-Present and Life time Version-Korean Version: K-SADS-PL) were used for diagnosis. The reliability and validity of the K-SADS-PL were previously determined (Kaufman et al. 1997; Kim et al. 2004). The full-range of The Korean Educational Development Institute-Wechsler Intelligence Scales for Children (KEDI-WISC) III (Park et al. 1996) was administered to each subject. Subjects were excluded if they had 1) any neurological disease or insult, developmental disorders including pervasive developmental disorders, or medical disorders that could affect brain development, 2) any history of substance abuse, psychotropic medication, significant fetal exposure to alcohol or drugs, or perinatal or neonatal complications, 3) full-scale Intelligence Quotients below 70, or 4) claustrophobia or irremovable metal materials. We recruited right-handed subjects only. Among 43 ADHD patients, 18 were excluded (13: subclinical ADHD, 2: brain abnormalities, 3: below 70 of IQ). At the baseline evaluation, a total of 25

ADHD subjects were included in the study. Among them, 5 subjects were additionally excluded in our analysis: 1 subject had poor adherence to medication (below 80% administration of prescribed medication according to self-reported medication administration chart), 1 subject had clinical suspicion of autism spectrum disorder rather than ADHD during clinical follow-up, and 3 subjects were loss to follow-up before twelfth week of treatment. Finally, 20 ADHD subjects completed the whole 12-week MPH treatment and MRI scanning at the end of the treatment. There was no significant difference in terms of age (Mann-Whitney U = 32.0, p = 0.221), IQ (Mann-Whitney U = 24.0, p = 0.077), K-ARS total score (Mann-Whitney U = 43.0, p = 0.749), Inattention score (Mann-Whitney U = 44.5, p = 0.830), Hyperactivity-impulsivity score (Mann-Whitney U = 41.0, p = 0.643) and K-CPRS score (Mann-Whitney U = 38.0, p = 0.498) between the included and excluded subjects. Among 28 TDC, one subject was excluded because of non-attendance at baseline evaluation. Finally, 20 psychotropic medication-naïve children with ADHD and 27 TDC were included in the further analysis. The imaging data used for this study was the expanded dataset from Choi et al. (2013).

Daejeon's St. Mary's Hospital Institutional Review Board approved all procedures. The purpose of the study was explained to the subjects and parents, who gave their written informed consent.

Clinical assessment and methylphenidate prescription

The severity of ADHD symptoms was evaluated with the Korean version of Dupaul's ADHD rating scale (K-ARS) at the first interview. The validity and reliability of K-ARS were established by So and colleagues (2002). In addition, the behavioral domains of each subject were rated by their parents using the Korean version of Conner's Parent Rating Scale (K-CPRS), for which the validity and reliability were determined in a previous study (Park et al. 2003).

After baseline R-fMRI acquisition, extended release form of MPH tablets (Concerta ®) was prescribed to 20 ADHD subjects. Two participants who addressed the problems of swallowing difficulty, were treated with Metadate CD ®. MPH doses were gradually titrated and adjusted to achieve desired symptom improvement for each subject while carefully monitored for adverse effects and drug compliance. The titration was limited if participants had intolerable side effects, or ADHD symptoms had been reduced to 'much improved' or 'very much improved' by the Clinical Global Impression – Global Improvement (CGI-I) scale. Symptom assessment and follow-up R-fMRI were acquired after twelve weeks later from the initial visit. The rating of the pre- and post-treatment states (PreTx and PostTx) of subjects and MPH prescription were conducted by an author. (J.C.).

Image acquisition

All images were acquired using a 1.5 T Philips scanner at Daejeon St. Mary's Hospital. Before starting the MR scan, the children were given time to adapt to the scanner environment. The subject's head was stabilized with cushions and taped to help minimize movement. The R-fMRI scan was acquired with an echo-planar imaging (EPI) sequence with the following imaging parameters: repetition time (TR) = 2000 ms; echo time (TE) = 35 ms; flip angle (FA) = 70°; voxel size =3.4375 × 3.4375 × 5 mm^3; imaging matrix =64 × 64; field-of-view (FOV) = 240 × 240 mm^2, number of volumes =210. The subjects were instructed to keep their eyes closed and not to think of anything particular during R-fMRI scans. A T1-weighted anatomical image was also acquired using a magnetization-prepared, gradient-echo sequence (TR = 25 ms; TE = 4.6 ms; FOV = 240 × 240 mm^2; voxel size = 1 × 1 × 1 mm^3). To relieve the subjects' anxiety, animation films were screened during structural MR scanning if they maintained minimal body movement. R-fMRI and structural MRI were acquired after twelve weeks of MPH treatment using the same scanner with identical scanning procedures and parameters. Because our study aimed to investigate short-term treatment effect among ADHD subjects whose symptoms were well-controlled by regular administration schedule, we scheduled PostTx MRI scanning conducted 2 h apart from MPH administration in the morning of the day of the scan.

Data preprocessing

The MRI data were preprocessed with the FMRIB Software Library (FSL, www.fmrib.ox.ac.uk/fsl) version 5.0, Analysis of Functional NeuroImages (http://afni.nimh.nih.gov/afni/), and the FreeSurfer image analysis suite (http://surfer.nmr.mgh.harvard.edu/) version 5.3. Preprocessing of R-fMRI data was performed sequentially with the following procedure. First, we discarded the initial five volumes from each R-fMRI data item to reduce T1 saturation effects. Rigid body transformation and slice timing correction were performed on the remaining 205 images using FSL software. After skull stripping, motion correction, removing of linear and quadratic trends, and band-pass filtering (0.01–0.1 Hz) of the R-fMRI data were performed to reduce physiological noise and signal drift using CompCor methods (Behzadi et al. 2007). Then, we applied spatial smoothing on all the valid voxels using a Gaussian kernel of 6 mm full-width at half-maximum. Next, R-fMRI volumes were registered with corresponding high-resolution T1-weighted images that had been co-registered to the Montreal Neurological Institute (MNI) T1 template.

Spatially-independent, global-level RSFN components were extracted using the Multivariate Exploratory Linear Optimized Decomposition into Independent Components

(MELODIC) module of the FSL software (Beckmann and Smith 2004). Multisession temporal concatenation in a MELODIC module was used to extract the probabilistic independent component (IC) for group analysis. A dual regression analysis was conducted to investigate the component-wise connectivity difference between groups. We used a publically available IC template suggested by Smith and colleagues, which had been proved to represent resting brain's functional dynamics across a large dataset (Smith et al. 2009). Among 20 RSFNs in the template, we selected 10 well-matched pairs of RSFNs which we considered as non-artefactual IC components. The RSFNs were used in further analysis as follows: left frontoparietal network (LFPN), right frontoparietal network (RFPN), central executive network (CEN), Sensory/Motor network (SM), auditory network (AN), default mode network (DMN), cerebellum (CBL), lateral visual processing network (LVN), medial visual processing network (MVN) and visual network-occipital pole (OVN).

Considering heterogeneity of the participants' ages and their unequal developmental stages, registration to a common standard 3D space would result in a biased transformation of a certain region. Rather than using the same approach used for a global-level approach, we adopted surface-based registration provided by the Freesurfer package. This approach reduced not only the inter-participant variability caused by the individual cortical folding pattern, but it also diminished the substantial spread of activation along the distant regions after spatial smoothing, which provided a critical advantage for local-level analysis. For this purpose, ALFF and fALFF were calculated from pre-processed R-fMRI data which were resampled into a 3 mm iso-voxel grid by averaging the square root of the power spectrum across 0.009–0.08 Hz and the power within the low-frequency range divided by the total power in the entire frequency range, respectively. Then, the high-resolution structural data of each participant were reconstructed to the cortical surface using methods based on the Freesurfer processing pipeline (Dale et al. 1999; Fischl and Dale 2000; Fischl et al. 1999a, b): registration to the Talairach atlas, bias field correction, skull stripping, intensity normalization, surface modeling, and spherical mapping and registration. ALFF and fALFF values in each cortical voxel were registered to the corresponding vertices in each subjects' surface model and spatial smoothing was applied to the surface vertices with a 5 mm full-width at half-maximum Gaussian kernel. Finally, Z-transformation of ALFF and fALFF from each subject space were performed and warped to the common spherical model called 'fsaverage' to compute group statistics.

Imaging data analysis

Functional connectivity analyses using dual regression were performed using time courses of the 10 RSFNs from each subject. (Filippini et al. 2009; Littow et al. 2010; Veer et al. 2010). Time course matrices from spatial IC maps in group ICA were used to estimate subjects-specific spatial maps, and then the connectivity difference from each RSFN was tested for statistical significance in a pairwise manner between the PreTx and PostTx ADHD groups. We also performed the same procedure to contrast PreTx and PostTx ADHD participants relative to TDC. Statistical analyses were conducted with 10,000 replicated permutation tests with the Threshold-Free Cluster Enhancement methods implemented in the FSL archive to reduce the possibility of error from arbitrary inference. Finally, we defined clusters that showed a family-wise error (FWE) corrected p-value less than 0.05 had significant functional connectivity.

Next, graph theoretical analysis among 10 RSFNs was conducted with the GRETNA toolbox (Wang et al. 2015), an open-source package built on Matlab program (Mathworks Inc.). From the mean time series data of 10 RSFNs, a partial correlation coefficient (PCC) was estimated between every two networks after controlling for the effect of other connections on them. We took absolute values from a negative PCC to quantify the connectivity strength and then constructed a graph network of each group with a 10 by 10 weighted matrix. We also assumed that those large-scale networks might interact with each other during the resting state. Thus, we analyzed only fully-connected networks ranging from a similarity threshold of 0.01 (dense connection) to 0.06 (scarce connection). The network characteristics used in the current study were as follows: clustering coefficient (CC), global and local efficiency (E_{global} and E_{local}), and modularity. The CC is the ratio of the number of existing connections to all possible connections of the subgraph connected to designated nodes (Onnela et al. 2005; Watts and Strogatz 1998), E_{global} and E_{local} are the inverse of the harmonic mean of the minimum path length within the entire network and all possible subgraphs, respectively (Latora and Marchiori 2001, 2003). Modularity is the difference of the expected edges between the intra-module and the inter-module, and the community structures of the module illustrated the group organizations of RSFNs (Newman 2006). For the network-wise comparison, each global metric was normalized using the mean and standard deviation of those from 1000 randomly generated graphs. Then, all properties of the ADHD group were compared in a pairwise manner and also contrasted with TDC by a two-sample t-test with a significance level of $p < 0.05$.

Finally, surface-based ALFF and fALFF analyses were performed with the general linear model implemented in the Freesurfer package. For estimating the MPH effect, we conducted a paired t-test between PreTx and PostTx data and then also compared each group with the TDC group, respectively. To reduce false results, we employed the cluster-forming

threshold at $p < 0.0001$, which was the conservative standard suggested in other studies (Silver et al. 2011), and all results were adjusted for FWE corrected $p < 0.05$ based on the 10,000 Monte-Carlo simulations.

All neuroimaging analyses were controlled for effects of demographic covariates including age, sex, and IQ.

Regression analysis with the random forest algorithm

The significant features extracted from the disparate R-fMRI analyses might be associated with clinical improvement of ADHD symptoms. However, conventional correlation analysis could only determine a one to one relationship between a single neuroimaging finding and symptom improvement, which is inappropriate for estimating integrative influence from multiple features. We adopted the random forest algorithm (Breiman 2001), an ensemble machine learning method, to explore the relationship between multiple neuroimaging features and clinical improvement. It operates by constructing a multitude of decision trees and expresses the role of a single feature, including weak and multivariate ones by the production of a feature-importance measure. In particular, the random forest algorithm has a considerable advantage in estimating high-order interactions and nonlinearity relationships between features (Strobl et al. 2009). In this framework, this approach provides an opportunity to explore minor features which might also be associated with clinical improvement. We tested the predictive power of all significant features from imaging analyses to explain clinical improvements measured from K-ARS and its inattention and hyperactivity-impulsivity subscale (K-ARS-I and K-ARS-H), and K-CPRS among 14 ADHD subjects who completed each symptom assessment (K-ARS and K-CPRS) both before and after twelve weeks of MPH treatment. To examine the paired difference after MPH administration, we normalized each participant's PostTx data using the respective mean and standard deviation of PreTx, then calculated difference between Z-transformed values. Clinical variables were transformed to percent change improvement from the PreTx state.

Regression analysis was conducted with the 'randomForestSRC' package implemented in R version 3.2.2. (RCoreTeam 2016), and the final results were summarized from 2000 bootstrap replicates to obtain a robust model that produced fewer error rates. Imaging features that had a smaller mean squared error than a randomly shuffled dataset were chosen as a significant predictor of symptom severity. The variable importance was calculated for each neuroimaging feature as the difference between out-of-bag error estimates from original bootstrapped trees and that of randomly permuted trees. Finally, we examined the effects of the demographic variables including age, sex, and IQ with random forest regression by adding them as explanatory variables to determine their effect on regression.

Results

Demographic characteristics

In the between-group analysis, there were no meaningful differences in age, height, and weight between the ADHD and TDC groups (Table 1). We recruited more boys than girls in both groups up to four-fold, but the proportion between the two groups did not differ from each other. In contrast, verbal, performance and full-scale IQ were significantly lower in participants with ADHD. In the ADHD group, 14 subjects were diagnosed as combined subtype ADHD, and six subjects were inattentive subtypes.

Average MPH dose at the twelfth week of treatment was 29.90 ± 13.56 mg (ranging from 18 mg to 72 mg). Treatment response to MPH was discernible when compared to the initial symptom assessment, and the total, inattention, and hyperactivity-impulsivity scores from K-ARS were significantly reduced to 17.87 ± 7.59 (paired $t = 10.34$, $p < 0.001$), 10.07 ± 4.15 (paired $t = 12.33$, $p < 0.001$), and 7.80 ± 4.26 (paired $t = 7.06$, $p < 0.001$), respectively. K-CPRS score also dropped to 10.14 ± 3.58 (paired $t = 9.10$, $p < 0.001$), which suggested marked symptom improvement after twelve weeks of MPH administration. According to the CGI-I rating, 18 ADHD subjects had met criteria for clinical response (10 subjects with 'very much improved', 8 subjects with 'much improved' and 2 subjects with 'minimally improved'), and 10 subjects had K-ARS total score of ≤18 which could be accounted as symptomatic remission at the twelfth week of treatment.

Table 1 Demographic and clinical characteristics of participants

	ADHD ($n = 20$)	TDC ($n = 27$)	t or χ^2
Age, y	10.60 ± 2.63	11.46 ± 2.40	−1.16
Male: Female, number	16:4	19:8	0.56
Height, cm	144.62 ± 16.05	147.66 ± 12.12	−0.73
Weight, kg	43.31 ± 19.12	43.92 ± 11.32	−0.14
Full scale IQ	97.3 ± 11.68	113.81 ± 12.44	−4.62***
Performance	95.25 ± 11.85	108.67 ± 15.36	−3.25**
Verbal	99.45 ± 12.59	114.15 ± 13.85	−3.74**
Father's education, y	14.78 ± 2.07	14.89 ± 2.31	−0.17
Mother's education, y	13.84 ± 1.95	14.41 ± 2.22	-0.89
K-ARS score, total	37.95 ± 9.14	6.22 ± 4.31	14.07***
Inattention	21.21 ± 4.24	4.26 ± 2.96	16.01***
Hyperactivity-Impulsivity	16.68 ± 6.01	1.96 ± 1.74	10.38***
K-CPRS score, total	20.53 ± 5.16	4.81 ± 4.59	10.86***

ADHD Attention-deficit/hyperactivity disorder, *TDC* Typically developing children, *K-ARS* Dupaul's ADHD rating scale, Korean version, *K-CPRS* Conner's parent rating scale, Korean version

** $p < 0.01$ *** $p < 0.001$

ICA with dual regression

In the ADHD group, LFPN connectivity to the left insula was significantly increased after MPH treatment and meaningful changes were also seen in intra-component areas, including the middle and dorsolateral prefrontal cortex (DLPFC) and part of the caudate nucleus (Table 2, Fig. 1a, Family-wise error corrected $p = 0.002$). In addition, connectivity between the RFPN and the pontine tegmentum of the brainstem was increased in PostTx state (Family-wise error corrected $p = 0.021$). However, we could not find any treatment-related decreased connectivity from any of the 10 RSFNs and other brain regions. Compared to the TDC group, the PreTx ADHD group showed reduced intra-component connectivity between the RFPN and bilateral precuneus and the right dorsolateral prefrontal cortex (Fig. 1b, Family-wise error corrected $p = 0.034$), and the PostTx ADHD group was found to have increased LFPN connectivity to the left insula, left DLPFC and left superior occipital area (Fig. 1c, Family-wise error corrected $p = 0.003$).

Graph theoretical analysis

Paired comparison of global metrics revealed that network-wise CC and E_{local} were significantly decreased after MPH treatment at a threshold of 0.05. The PostTx group also showed reduced CC of LFPN (threshold of 0.02), CBL (threshold of 0.05), and OVN (threshold of 0.06) among nodal metrics (Table 2, Fig. 2a, b). Global graph metrics of PreTx group did not differ from the TDC group, but the nodal metrics analysis showed elevated CC of LPFN (threshold of 0.04) and E_{local} of DMN (threshold ranged from 0.02 to 0.04). Under MPH treatment, a lower global CC was identified at a threshold ranging from 0.03 to 0.05), as well as a reduced CC of OVN (threshold of 0.06) and CBL (threshold of 0.05 and 0.06), and E_{local} of CBL (threshold ranged from 0.04 to 0.06). We could not find any meaningful differences in modularity and E_{global} in all the between-group comparisons. However, a qualitative investigation of community structure illustrated that functional integration of LFPN to DMN after MPH treatment at a threshold of 0.01 and 0.02, which was also found in the TDC group (Fig. 2c).

ALFF and fALFF analysis

In a pairwise analysis of the ADHD group, surface clusters in the bilateral superior parietal cortex (SPC) showed reduced ALFF, while regions including the right inferior temporal gyrus (ITG), right temporal pole and inferior frontal gyrus (IFG) had an increased ALFF after MPH treatment (Table 2, Fig. 3a). However, paired analysis of fALFF did not reach the levels of statistical significance after correction for multiple comparisons. In addition, we could not find any significant changes from PreTx ADHD children relative to the controls. Meanwhile, PostTx ADHD group had an increased ALFF in the left DLPFC relative to TDC, (Fig. 3b), and a decreased fALFF in the right superior frontal gyrus as well as an increased fALFF in the left orbitofrontal and right ITG (Fig. 3c).

Imaging features explaining clinical variables

Among the 14 ADHD subjects, significant changes across five local and large-scale RSFNs could explain the 27.1% variance of symptom improvement measured by the K-ARS total score (Fig. 4). The highest variable importance was found in a reduced ALFF in the right SPC (15.35%), followed by an ALFF change in the left SPC (6.69%) decreased network-wise E_{local} (6.39%), CC of CBL (4.95%) and network-wise CC (2.52%). A combination of those features also had predictive power for both K-ARS-I (13.85%) and K-ARS-H (32.95%), and the most important feature explaining K-ARS-I and K-ARS-H was the ALFF changes in the left (11.84%) and right SPC (31.31%), respectively. In addition, 13.72% of K-CPRS improvement could be explained by collaboration of neuroimaging features consisting of a reduced network-wise CC (8.64%), ALFF in the right IFG (7.65%), CC of CBL (5.83%), ALFF in the right ITG (3.12%) and the right SPC (0.59%). However, we could not identify the contribution of other significant neuroimaging features in symptom improvement. Features with higher importance tended to have a linear relationship with the clinical outcome in the partial correlation analysis, but a meaningful contribution of non-linear predictors was also found.

In all regression analyses, inclusion of age, sex and IQ resulted in a loss of predictive power (K-ARS total score, 21.68%; K-ARS-I 1.22%; K-ARS-H, 28.21%, K-CPRS, 4.51% variance explained with demographic variables), which indicated that clinical improvements were not meaningfully affected by demographic characteristics of the participants.

Discussion

Our study investigated the local and large-scale changes in the RSFN after MPH administration and their integrative influence on symptom improvement. Using ICA with dual regression and graph theoretical analysis, we revealed treatment relevant alterations in large-scale connectivity which increased the LFPN connectivity to the left insular and frontal cortex, increased the RFPN connectivity to the brainstem, decreased CC in the LFPN, CBL, OVN and overall network. In addition, localized changes were presented both as decreased ALFF over the superior parietal cortex and elevated ALFF in the right IFG and ITG. With the random forest algorithm, the subset of neuroimaging features could explain the

Table 2 Significant results from all three resting-state fMRI analysis among pre- and post-treatment ADHD group and typically developing children

PreTx vs. PostTx					PreTx vs. TDC					PostTx vs. TDC				
ICA with dual regression														
Contrast	Network	Regions	MNI coordinates	p*	Contrast	Network	Regions	MNI coordinates	p*	Contrast	Network	Regions	MNI coordinates	p*
PostTx > PreTx	LFPN	Left insula	−38, 2, 6	0.002	TDC > PreTx	RFPN	Bilateral precuneus	0, −48, 40	0.034	PostTx > TDC	LFPN	Left insula	−38, 2, 6	0.003
		Left middle frontal cortex	−36, 26,46 −48, 38, 16				Right dorsolateral prefrontal cortex	40, 26, 44				Occipital pole	−8, −90, 22	
		Left dorsolateral prefrontal cortex										Left middle frontal cortex	−38, 8, 44	
	RFPN	Brainstem	−6, −32, −42	0.021										
Graph theoretical analysis														
Contrast	Network	measure	Cost	p	Contrast	Network	Measure	Cost	p	Contrast	Network	Measure	Cost	p
PreTx > PostTx	LFPN	CC	2	0.037	PreTx > TDC	LPFN	CC	4	0.047	TDC > PostTx	CBL	E_{local}	4	0.009
	CBL	CC	5	0.031		DMN	E_{local}	2	0.004		CBL	E_{local}	5	0.011
	OVN	CC	6	0.043		DMN	E_{local}	3	0.012		CBL	E_{local}	6	0.010
	Network	CC	5	0.025		DMN	E_{local}	4	0.013		CBL	CC	5	0.032
	Network	E_{local}	5	0.050							CBL	CC	6	0.034
											OVN	CC	6	0.046
											Network	CC	3	0.046
											Network	CC	4	0.023
											Network	CC	5	0.021
ALFF and fALFF														
Contrast	Measure	Region	MNI coordinates	p*	Contrast	Measure	Region	MNI coordinates	p*	Contrast	Measure	Region	MNI coordinates	p*
PreTx > PostTx	ALFF	Left superior parietal	−9, −90, 29	<0.001	No significant results					PostTx > TDC	ALFF	Left middle frontal	−37, 10, 35	<0.001
	ALFF	Right superior parietal	21, −83, 40	0.001							fALFF	Left inferior temporal	−48, −16, −36	<0.001
PostTx > PreTx	ALFF	Right inferior temporal	39, −5, −39	<0.001							fALFF	Right orbitofrontal	13, 31, −25	0.008
	ALFF	Right temporal pole	34, −1, −21	<0.001						TDC > PostTx	fALFF	Right superior frontal	10, 58, 4	0.006
	ALFF	Right frontal pole	15, 58, −16	0.046										

PreTx Pre-treatment ADHD, *PostTx* Post-treatment ADHD, *TDC* Typically developing children, *ICA* Independent component analysis, *MNI* Montreal Neurological Institute, *LFPN* Left fronto-parietal network, *RFPN* Right fronto-parietal network, *CBL* Cerebellum, *OVN* Occipital pole visual network, *DMN* Default mode network, *CC* Clustering coefficient, E_{local} Local efficiency, *ALFF* Amplitude of low frequency fluctuation; fALFF, fractional ALFF

*Family-wise error corrected *p* value

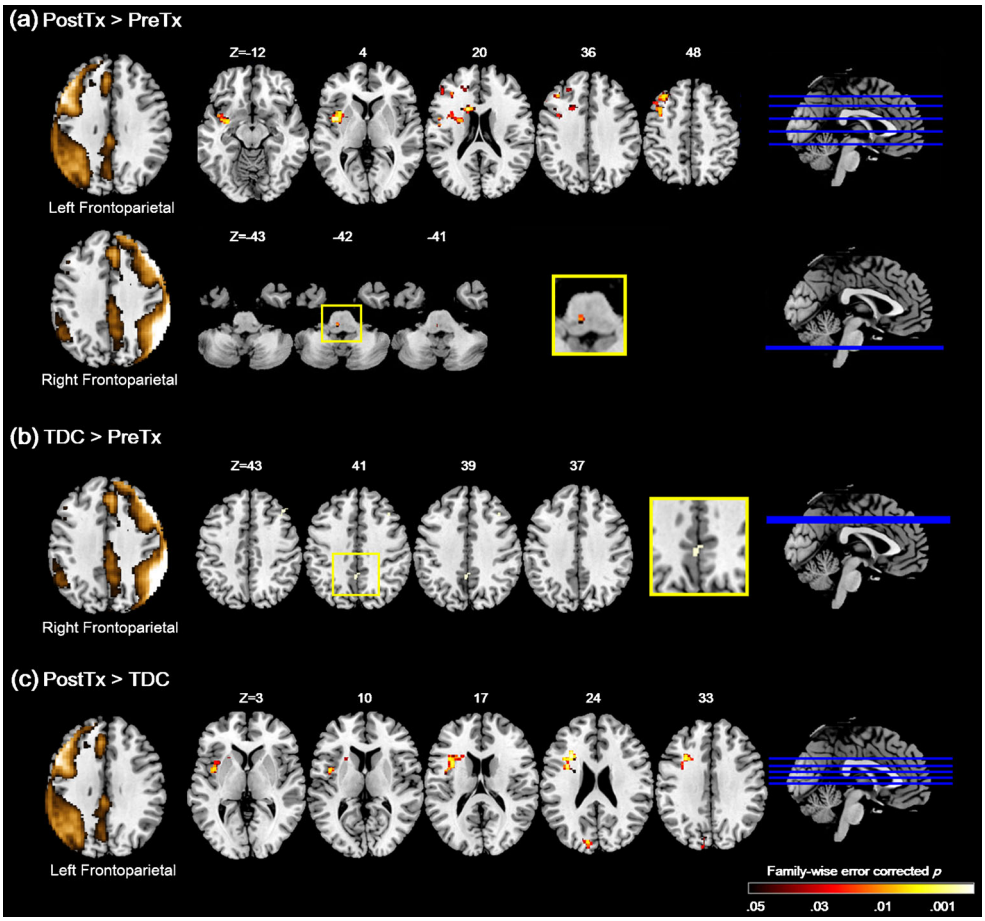

Fig. 1 Large-scale connectivity changes identified from dual regression analysis. (**a**) Paired analysis before and after 1-month MPH treatment. Increased connectivity was found between left frontoparietal network and left insula and dorsolateral prefrontal cortex as well as right frontoparietal network and pontine reticular area after treatment. (**b**) Strong right frontoparietal network connectivity to precuneus and right dorsolateral prefrontal cortex was found in typically developing children relative to medication-naïve ADHD group. (**c**) After treatment, ADHD group showed increased left frontoparietal connectivity to left insula and dorsolateral prefrontal cortex than typically developing children. PreTx, pre-treatment ADHD; PostTx, post-treatment ADHD; TDC, typically developing children

considerable variance of symptom improvement measured by K-ARS and K-CPRS after twelve weeks of MPH treatment.

Dual regression results revealed that the PostTx group was associated with increased connectivity between the LFPN and the left insula relative to both treatment-naïve ADHD and TDC. Current results were parallel with previous studies in which activity and connectivity within the ventrolateral prefrontal cortex (including insula) were upregulated by MPH treatment (Sripada et al. 2013; Cubillo et al. 2014; Mueller et al. 2014). The insular cortex is a hub region of the SN that plays a pivotal role in allocating resources between the frontoparietal network and the DMN to elicit adaptive responses (Dosenbach et al. 2007). In view of the decreased or immature connectivity between the SN and the frontoparietal network in the ADHD group (Choi et al. 2013; Sidlauskaite et al. 2016; Sripada et al. 2014), our finding might indicate upregulation of the hypoconnected intrinsic network by MPH-induced endogenous dopamine stimulation (Arnsten and Pliszka 2011). In addition, the left DLPFC and caudate nucleus also showed increased intra-component connectivity, which is strongly linked to executive function deficit in ADHD (Castellanos et al. 2006). It is consistent with the previous finding that regional blood flow of those regions increased after MPH treatment (Kim et al. 2001). Another noteworthy finding in the pairwise comparison was increased RFPN connectivity to the ascending reticular activation system (ARAS). The ARAS plays a key role in arousal and attention (Paus 2000), which has abundant noradrenergic projections from locus coeruleus (Sarter et al. 2006; Broyd et al. 2005). Thus, enhanced connectivity strength to the ARAS might be attributed to the noradrenergic facilitation effect by MPH. Additionally, the PreTx group showed decreased intra-component connectivity in a small part of the precuneus and right DLPFC relative to TDC, while this difference disappeared after treatment. Our findings might support the idea that MPH-induced recovery of diminished regional connectivity between the DMN and the frontoparietal network, which was suggested in a previous study (Sripada et al. 2013).

In graph theoretical analysis, a decrease in global network connectivity (network-wise CC and E_{local}) was identified in the PostTx group, relative to the PreTx and TDC groups. In addition, the nodal CC also decreased in LFPN, CBL and OVN after treatment. Recent literature suggested that the ADHD group had a higher average connectivity in the subnetwork towards the regular graph during the resting state (Silk et al. 2016; Wang et al. 2009), but aberrant connections were downregulated by MPH treatment (Silk et al. 2016). In addition, ADHD subjects showed enhanced CBL connectivity

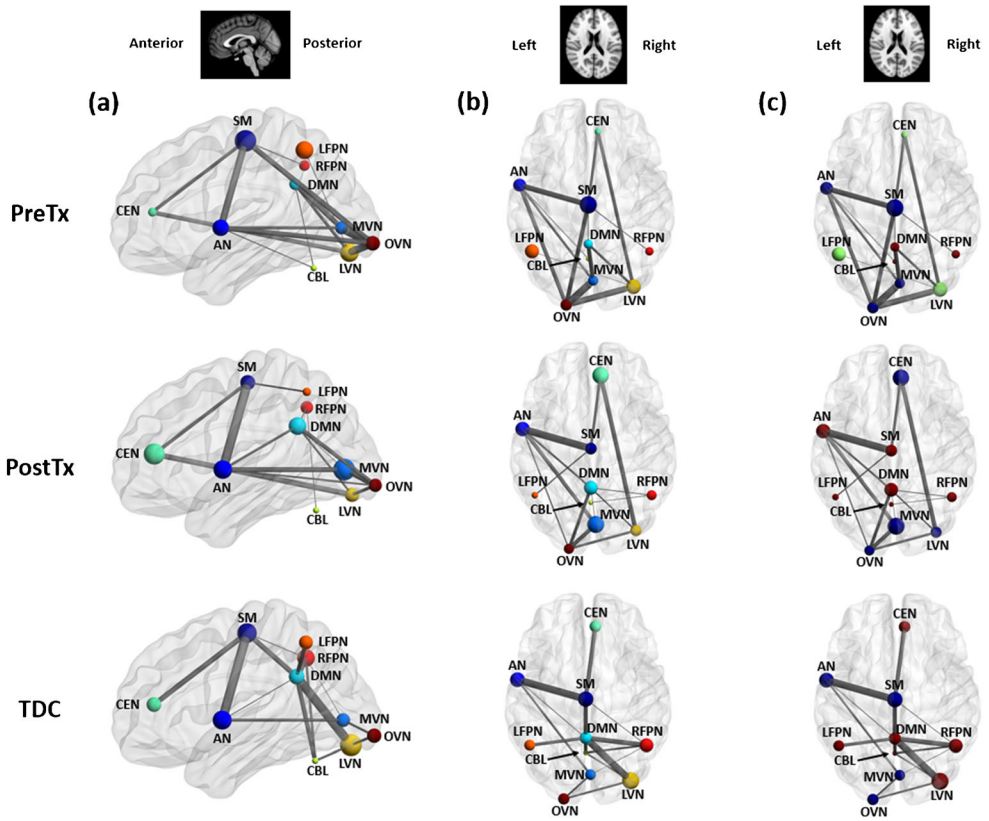

Fig. 2 Large-scale intrinsic functional networks form graph theoretical analysis at similarity threshold 0.02. (**a**) and (**b**) Sagittal and axial view of clustering coefficient map among pre- and post-treatment ADHD and typically developing children. Significant difference was found in left frontoparietal networks. (**c**) Community structure of graph theoretical networks. Post-treatment ADHD group showed integration of left frontoparietal networks likewise typically developing children. PreTx, pre-treatment ADHD; PostTx, post-treatment ADHD; TDC, typically developing children; LFPN, Left frontoparietal network; RFPN, Right frontoparietal network; CEN, Central executive network; SM, Sensory/Motor network; AN, Auditory network; DMN, Default mode network; CBL, Cerebellum; LVN, Lateral visual processing network; MVN, Medial visual processing network; OVN, Visual network-occipital pole

to the frontoparietal and visual networks (Kucyi et al. 2015), while recent studies demonstrated that MPH treatment normalized regional connectivity in the fronto-parietal, CBL and visual networks (Yang et al. 2016; Mueller et al. 2014; Rosenberg et al. 2016; Sripada et al. 2013). Taking all the evidence into account, our findings support the previous hypothesis that functional improvement might be associated with MPH-induced functional segregation of the resting network (Sripada et al. 2013; Yang et al. 2016). Resting connectivity suppression by MPH was also found in a comparison between the PostTx and TDC groups. Meanwhile, our study also illustrated a functional integration of the LFPN after MPH treatment, although we could not find any quantitative change in modularity. Our finding could be interpreted as a delayed consolidation DMN over development in ADHD, which was suggested in previous studies (Fair et al. 2010; Castellanos et al. 2006) In addition, MPH treatment might have a differential effect on a resting network, including functional segregation across the global network as well as reorganization of a unified module linked to the DMN.

MPH treatment also modulated local spontaneous activity in the bilateral SPC, right IFG, and right ITG. In addition, the PostTx group also showed increased ALFF in the IFG, ITG, and DLPFC relative to the TDC. Our findings are generally corroborated by the results from An et al. that suggested that a single administration of MPH had resulted in an increased ReHo in the orbital and inferior frontal area and a decreased ReHo in the superior parietal cortex compared with a placebo (An et al. 2013b). As previous studies pointed out that the right IFG is the key region for response inhibition, sustained attention and attentional control for relevant stimulus (Hampshire et al. 2010). The inferior to middle temporal cortex have been less associated with ADHD pathophysiology, but greater activation of those regions have been shown to be related to low response time variability (Spinelli et al. 2011). In addition, MPH elicited downregulation of the bilateral SPC regions, which was significantly correlated with improvement of symptom severity and attentional performance (An et al. 2013b; Cho et al. 2007; Kim et al. 2012). Taking that evidence into account, we can consider that the normalization of baseline hyperactivity in SPC and upregulation of IFG, DLPFC and ITG might be

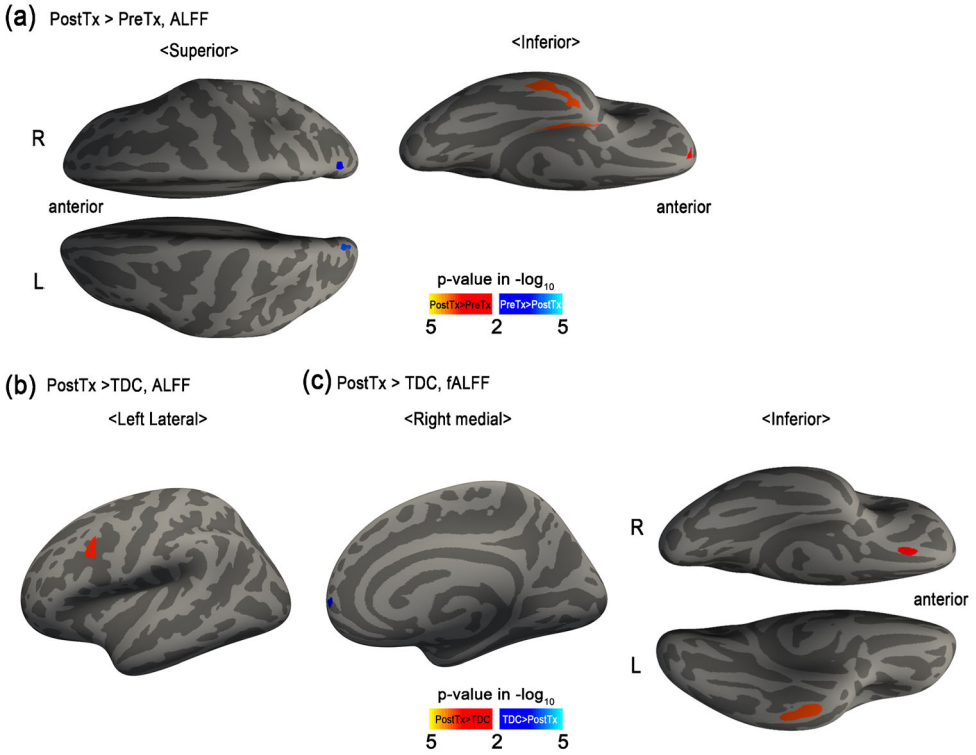

Fig. 3 Local resting-state activity difference using ALFF/fALFF approach. (**a**) Pairwise comparison revealed ALFF reduction in bilateral superior parietal cortex while significant activity enhancement was found in right inferior frontal and temporal area. (**b**) ALFF of left DLPFC was also found to be increased in ADHD with MPH treatment group. (**c**) Post-treatment ADHD group showed decreased fALFF in right medial orbitofrontal cortex relative to typically developing children and increased fALFF in right inferior frontal and left inferior temporal cortex. PreTx, pre-treatment ADHD; PostTx, post-treatment ADHD; TDC, typically developing children; ALFF, Amplitude of low frequency fluctuation; fALFF, fractional amplitude of low frequency fluctuation

associated with recovery of the attentional processing network. We could not find a significant ALFF/fALFF difference between the TDC and PreTx groups as previous studies reported (An et al. 2013a; Zang et al. 2007). Negative results could be driven by a small kernel size for spatial smoothing or a robust threshold for multiple comparison corrections relative to

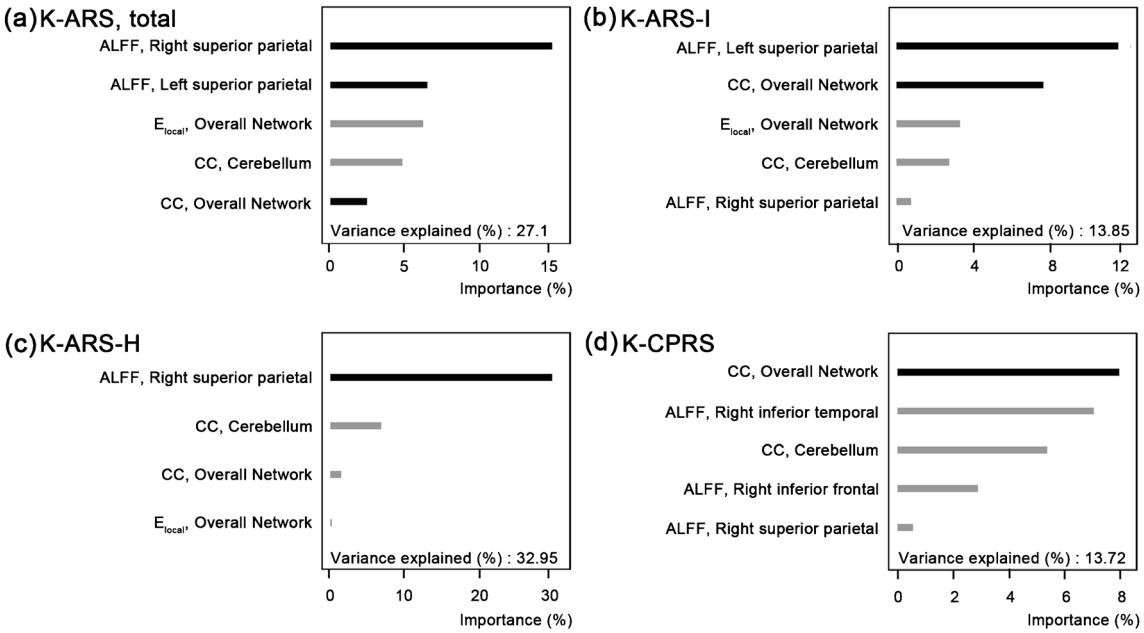

Fig. 4 Estimated feature importance for clinical improvement and summarized explanatory power from random Forest regression in ADHD group. Feature importance and explanatory power has been demonstrated for explaining (**a**) total K-ARS score, (**b**) Inattentive domain score of K-ARS, (**c**) Hyperactivity/Impulsivity domain score of K-ARS and (d) K-CPRS. Features colored in black had significance level of $p < 0.05$, while those colored in gray did not show significance in Spearman's rank order correlation analysis. K-ARS, Dupaul's ADHD rating scale, Korean version; K-ARS-I, Inattentive domain score of K-ARS; K-ARS-H, Hyperactivity/Impulsivity domain score of K-ARS; K-CPRS, Conner's parent rating scale, Korean version; CC, Clustering coefficient; E_{local}, Local efficiency

previous studies. Furthermore, comparison upon a two-dimension surface could provide better test-retest reliability using improved intra- and inter-subject registration quality (Zuo et al. 2013); however, the key structures for ADHD, including the striatum and cerebellum, cannot be covered in a surface mask. Therefore, local spontaneous activity differences between ADHD and TDC would need further exploration.

In the multivariate regression analysis, a considerable variance of K-ARS and K-CPRS was explained by the collaboration of neuroimaging features from both local and large-scale RSFNs. ALFF changes in the bilateral SPC had greater importance in predicting changes of the K-ARS and subdomain score. The contribution of the network-wise CC was prominent in explaining K-CPRS and also associated with K-ARS improvement. The included features and their importance were different between K-ARS and K-CPRS, which might be derived from rater's characteristics (trained clinician vs. parent) and categories of assessment (symptoms in the DSM-IV diagnostic criteria vs. general childhood behavioral problems). High importance features tended to have a linear relationship in the partial correlation analysis, which might suggest a robust association between the recovery of intrinsic functional connectivity and clinical improvement. Furthermore, our approach could also reveal the substantial role of features with the minor importance that could not be detected in the conventional analysis that depended on a linearity assumption. Converging evidence suggested that dysfunctions associated with ADHD pathophysiology encompass both a number of large-scale and local changes in RSFNs which are largely interconnected to each other (Castellanos and Proal 2012; Di et al. 2013; Zang et al. 2007). In that sense, our approach might suggest the joint influence from diverse RSFN features on symptom improvement. However, some features, including large-scale changes in LFPN, RFPN and OVN connectivity, did not have any importance in predicting therapeutic effects. Fronto-parietal and visual networks have been implicated in ADHD pathophysiology, but impairments of such networks were identified mostly from task-based fMRI studies (Rubia et al. 2011; Silk et al. 2008). Thus, changes in a task-positive network might have limited influence on the intrinsic functional organization, as well as predicting symptom improvement. Finally, any explanatory benefit from including the age, sex and IQ might suggest that major symptom improvement was attributed to MPH-induced RSFN alteration, rather than subjects' demographic characteristics.

To our knowledge, this is the first study to use multi-level R-fMRI analysis to explore MPH effect in ADHD subjects. In addition, machine learning application to R-fMRI data analysis showed promising results that could estimate the relationship between complex neuroimaging findings and subsequent clinical symptom improvement. However, there are some limitations to be declared of our study. First, the sample size of 20 ADHD and 27 TDC was relatively small, which limited generalization of our findings. In addition, a small number of subjects (n = 14) in random forest regression analysis could lower the performance of decision tree algorithm because of underestimation of the interrelationship among features. Second, a particular form of MPH was administered to ADHD participants as open-label, and the study protocol did not include a randomization process and/or a placebo-controlled group. This might confound symptom assessment to a favorable outcome after MPH treatment. Third, functional changes found in our analysis might be driven partly by pharmacodynamic properties of MPH, rather than recovery of symptoms. However, the study design constrained the inclusion of the TDC group with MPH treatment because of ethical considerations. Finally, most analyses in our study targeted the functional changes in the cortex; thus, subcortical contributions to clinical improvement could not be estimated. Further study with improved design will be needed to overcome these issues.

Conclusion

This study investigated both large-scale and localized RSFN changes in ADHD subjects after twelve weeks of MPH treatment. Furthermore, we estimated the integrated effects of multi-dimensional changes across RSFNs to clinical improvement with a novel ensemble learning algorithm. Among subsequent changes elicited by MPH, features strongly associated with K-ARS improvement increased local spontaneous activity in the bilateral SPC, reduced the CC of the global network and CBL. In addition, we predicted K-CPRS from a combination of reduced network-wise connectivity and normalized baseline activity across the right frontal, temporal, and parietal cortex. Our findings suggested that the neural mechanism of symptom improvement by MPH treatment could be associated with alteration of spontaneous activity in the SPC or widespread brain regions as well as functional segregation of the large-scale intrinsic functional network.

Compliance with ethical standards

Funding This research was supported by the Brain Research Program through the National Research Foundation of Korea (NRF) funded by the Ministry of Science, ICT & Future Planning (NRF-2016M3C7A1914448 to B.J.), and by KAIST Future Systems Healthcare Project from the Ministry of Education, Science and Technology (N11160068 to B.J.)

Conflict of interest All authors declares that they have no conflict of interest.

Ethical approval All procedures performed in studies involving human participants were in accordance with the ethical standards of the institutional and/or national research committee and with the 1964 Helsinki declaration and its later amendments or comparable ethical standards.

Informed consent Informed consent was obtained from all individual participants and their parents included in the study.

References

An, L., Cao, X. H., Cao, Q. J., Sun, L., Yang, L., Zou, Q. H., et al. (2013b). Methylphenidate normalizes resting-state brain dysfunction in boys with attention deficit hyperactivity disorder. *Neuropsychopharmacology, 38*(7), 1287–1295. doi:10.1038/npp.2013.27.

An, L., Cao, Q. J., Sui, M. Q., Sun, L., Zou, Q. H., Zang, Y. F., et al. (2013a). Local synchronization and amplitude of the fluctuation of spontaneous brain activity in attention-deficit/hyperactivity disorder: a resting-state fMRI study. *Neuroscience Bulletin, 29*(5), 603–613. doi:10.1007/s12264-013-1353-8.

Arnsten, A. F., & Pliszka, S. R. (2011). Catecholamine influences on prefrontal cortical function: relevance to treatment of attention deficit/hyperactivity disorder and related disorders. *Pharmacology, Biochemistry, and Behavior, 99*(2), 211–216. doi:10.1016/j.pbb.2011.01.020.

Beckmann, C. F., & Smith, S. M. (2004). Probabilistic independent component analysis for functional magnetic resonance imaging. *IEEE Transactions on Medical Imaging, 23*(2), 137–152. doi:10.1109/TMI.2003.822821.

Behzadi, Y., Restom, K., Liau, J., & Liu, T. T. (2007). A component based noise correction method (CompCor) for BOLD and perfusion based fMRI. *NeuroImage, 37*(1), 90–101. doi:10.1016/j.neuroimage.2007.04.042.

Berridge, C. W., Devilbiss, D. M., Andrzejewski, M. E., Arnsten, A. F., Kelley, A. E., Schmeichel, B., et al. (2006). Methylphenidate preferentially increases catecholamine neurotransmission within the prefrontal cortex at low doses that enhance cognitive function. *Biological Psychiatry, 60*(10), 1111–1120. doi:10.1016/j.biopsych.2006.04.022.

Breiman, L. (2001). Random forests. *Machine Learning, 45*(1), 5–32. doi:10.1023/A:1010933404324.

Broyd, S. J., Johnstone, S. J., Barry, R. J., Clarke, A. R., McCarthy, R., Selikowitz, M., et al. (2005). The effect of methylphenidate on response inhibition and the event-related potential of children with attention deficit/hyperactivity disorder. *International Journal of Psychophysiology, 58*(1), 47–58. doi:10.1016/j.ijphyscho.2005.03.008.

Bullmore, E., & Sporns, O. (2009). Complex brain networks: Graph theoretical analysis of structural and functional systems. *Nature Reviews. Neuroscience, 10*(3), 186–198. doi:10.1038/nrn2575.

Castellanos, F. X., & Aoki, Y. (2016). Intrinsic functional connectivity in attention-deficit/hyperactivity disorder: a Science in development. *Biol Psychiatry Cogn Neurosci Neuroimaging, 1*(3), 253–261. doi:10.1016/j.bpsc.2016.03.004.

Castellanos, F. X., & Proal, E. (2012). Large-scale brain systems in ADHD: beyond the prefrontal-striatal model. *Trends in Cognitive Sciences, 16*(1), 17–26. doi:10.1016/j.tics.2011.11.007.

Castellanos, F. X., Sonuga-Barke, E. J., Milham, M. P., & Tannock, R. (2006). Characterizing cognition in ADHD: beyond executive dysfunction. *Trends in Cognitive Sciences, 10*(3), 117–123. doi:10.1016/j.tics.2006.01.011.

Cho, S. C., Hwang, J. W., Kim, B. N., Lee, H. Y., Kim, H. W., Lee, J. S., et al. (2007). The relationship between regional cerebral blood flow and response to methylphenidate in children with attention-deficit hyperactivity disorder: comparison between non-responders to methylphenidate and responders. *Journal of Psychiatric Research, 41*(6), 459–465. doi:10.1016/j.jpsychires.2006.05.011.

Choi, J., Jeong, B., Lee, S. W., & Go, H. J. (2013). Aberrant development of functional connectivity among resting state-related functional networks in medication-naive ADHD children. *PloS One, 8*(12), e83516. doi:10.1371/journal.pone.0083516.

Cubillo, A., Smith, A. B., Barrett, N., Giampietro, V., Brammer, M. J., Simmons, A., et al. (2014). Shared and drug-specific effects of atomoxetine and methylphenidate on inhibitory brain dysfunction in medication-naive ADHD boys. *Cerebral Cortex, 24*(1), 174–185. doi:10.1093/cercor/bhs296.

Czerniak, S. M., Sikoglu, E. M., King, J. A., Kennedy, D. N., Mick, E., Frazier, J., et al. (2013). Areas of the brain modulated by single-dose methylphenidate treatment in youth with ADHD during task-based fMRI: a systematic review. *Harvard Review of Psychiatry, 21*(3), 151–162. doi:10.1097/HRP.0b013e318293749e.

Dale, A. M., Fischl, B., & Sereno, M. I. (1999). Cortical surface-based analysis. I. Segmentation and surface reconstruction. *Neuroimage, 9*(2), 179–194. doi:10.1006/nimg.1998.0395.

Di, X., Kim, E. H., Huang, C. C., Tsai, S. J., Lin, C. P., & Biswal, B. B. (2013). The influence of the amplitude of low-frequency fluctuations on resting-state functional connectivity. *Frontiers in Human Neuroscience, 7*, 118. doi:10.3389/fnhum.2013.00118 .

Dosenbach, N. U., Fair, D. A., Miezin, F. M., Cohen, A. L., Wenger, K. K., Dosenbach, R. A., et al. (2007). Distinct brain networks for adaptive and stable task control in humans. *Proceedings of the National Academy of Sciences of the United States of America, 104*(26), 11073–11078. doi:10.1073/pnas.0704320104.

DuPaul, G. J., McGoey, K. E., Eckert, T. L., & VanBrakle, J. (2001). Preschool children with attention-deficit/hyperactivity disorder: impairments in behavioral, social, and school functioning. *Journal of the American Academy of Child and Adolescent Psychiatry, 40*(5), 508–515. doi:10.1097/00004583-200105000-00009.

Epstein, J. N., Casey, B. J., Tonev, S. T., Davidson, M. C., Reiss, A. L., Garrett, A., et al. (2007). ADHD- and medication-related brain activation effects in concordantly affected parent-child dyads with ADHD. *Journal of Child Psychology and Psychiatry, 48*(9), 899–913. doi:10.1111/j.1469-7610.2007.01761.x.

Fair, D. A., Nigg, J. T., Iyer, S., Bathula, D., Mills, K. L., Dosenbach, N. U., et al. (2012). Distinct neural signatures detected for ADHD subtypes after controlling for micro-movements in resting state functional connectivity MRI data. *Frontiers in Systems Neuroscience, 6*, 80. doi:10.3389/fnsys.2012.00080.

Fair, D. A., Posner, J., Nagel, B. J., Bathula, D., Dias, T. G., Mills, K. L., et al. (2010). Atypical default network connectivity in youth with attention-deficit/hyperactivity disorder. *Biological Psychiatry, 68*(12), 1084–1091. doi:10.1016/j.biopsych.2010.07.003.

Filippini, N., MacIntosh, B. J., Hough, M. G., Goodwin, G. M., Frisoni, G. B., Smith, S. M., et al. (2009). Distinct patterns of brain activity in young carriers of the APOE-epsilon4 allele. *Proceedings of the National Academy of Sciences of the United States of America, 106*(17), 7209–7214. doi:10.1073/pnas.0811879106.

Fischl, B., & Dale, A. M. (2000). Measuring the thickness of the human cerebral cortex from magnetic resonance images. *Proceedings of the National Academy of Sciences of the United States of America, 97*(20), 11050–11055. doi:10.1073/pnas.200033797.

Fischl, B., Sereno, M. I., & Dale, A. M. (1999a). Cortical surface-based analysis. II: inflation, flattening, and a surface-based coordinate system. *NeuroImage, 9*(2), 195–207. doi:10.1006/nimg.1998.0396.

Fischl, B., Sereno, M. I., Tootell, R. B., & Dale, A. M. (1999b). High-resolution intersubject averaging and a coordinate system for the cortical surface. *Human Brain Mapping, 8*(4), 272–284.

Hampshire, A., Chamberlain, S. R., Monti, M. M., Duncan, J., & Owen, A. M. (2010). The role of the right inferior frontal gyrus: inhibition and attentional control. *NeuroImage, 50*(3), 1313–1319. doi:10.1016/j.neuroimage.2009.12.109.

Kaufman, J., Birmaher, B., Brent, D., Rao, U., Flynn, C., Moreci, P., et al. (1997). Schedule for affective disorders and Schizophrenia for school-age children-present and lifetime version (K-SADS-PL): initial reliability and validity data. *Journal of the American Academy of Child and Adolescent Psychiatry, 36*(7), 980–988. doi:10.1097/00004583-199707000-00021.

Kim, Y. S., Cheon, K. A., Kim, B. N., Chang, S. A., Yoo, H. J., Kim, J. W., et al. (2004). The reliability and validity of kiddie-schedule for

affective disorders and Schizophrenia-present and lifetime version-Korean version (K-SADS-PL-K). *Yonsei Medical Journal, 45*(1), 81–89.

Kim, B. N., Lee, J. S., Cho, S. C., & Lee, D. S. (2001). Methylphenidate increased regional cerebral blood flow in subjects with attention deficit/hyperactivity disorder. *Yonsei Medical Journal, 42*(1), 19–29. doi:10.3349/ymj.2001.42.1.19.

Kim, J., Whyte, J., Patel, S., Europa, E., Wang, J., Coslett, H. B., et al. (2012). Methylphenidate modulates sustained attention and cortical activation in survivors of traumatic brain injury: a perfusion fMRI study. *Psychopharmacology, 222*(1), 47–57. doi:10.1007/s00213-011-2622-8.

Konrad, K., Neufang, S., Fink, G. R., & Herpertz-Dahlmann, B. (2007). Long-term effects of methylphenidate on neural networks associated with executive attention in children with ADHD: results from a longitudinal functional MRI study. *Journal of the American Academy of Child and Adolescent Psychiatry, 46*(12), 1633–1641. doi:10.1097/chi.0b013e318157cb3b.

Kucyi, A., Hove, M. J., Biederman, J., Van Dijk, K. R., & Valera, E. M. (2015). Disrupted functional connectivity of cerebellar default network areas in attention-deficit/hyperactivity disorder. *Human Brain Mapping, 36*(9), 3373–3386. doi:10.1002/hbm.22850.

Latora, V., & Marchiori, M. (2001). Efficient behavior of small-world networks. *Physical Review Letters, 87*(19), 198701. doi:10.1103/PhysRevLett.87.198701.

Latora, V., & Marchiori, M. (2003). Economic small-world behavior in weighted networks. *European Physical Journal B, 32*(2), 249–263. doi:10.1140/epjb/e2003-00095-5.

Littow, H., Elseoud, A. A., Haapea, M., Isohanni, M., Moilanen, I., Mankinen, K., et al. (2010). Age-related differences in functional nodes of the brain cortex - a high model order group ICA study. *Frontiers in Systems Neuroscience, 4,* doi:10.3389/fnsys.2010.00032.

Mueller, S., Costa, A., Keeser, D., Pogarell, O., Berman, A., Coates, U., et al. (2014). The effects of methylphenidate on whole brain intrinsic functional connectivity. *Human Brain Mapping, 35*(11), 5379–5388. doi:10.1002/hbm.22557.

Newman, M. E. (2006). Modularity and community structure in networks. *Proceedings of the National Academy of Sciences of the United States of America, 103*(23), 8577–8582. doi:10.1073/pnas.0601602103.

Onnela, J. P., Saramaki, J., Kertesz, J., & Kaski, K. (2005). Intensity and coherence of motifs in weighted complex networks. *Physical Review. E, Statistical, Nonlinear, and Soft Matter Physics, 71*(6 Pt 2), 065103. doi:10.1103/PhysRevE.71.065103.

Park K. S. Y. J., Park H. J., Kwon K. U. (1996). *Development of KEDI-WSIC, individual intelligence test for Korean children* Seoul: Korean educational development institute

Park, E., So, Y., Kim, Y., Choi, N., Kim, S., Noh, J., et al. (2003). The reliability and validity of Korean conners parent and teacher rating scale. *Korean Journal of Child and Adolescent Psychiatry, 14*(2), 183–196.

Paus, T. (2000). Functional anatomy of arousal and attention systems in the human brain. *Progress in Brain Research, 126*, 65–77. doi:10.1016/S0079-6123(00)26007-X.

R Core Team (2016). *R: a language and environment for statistical computing*. Vienna, Austria: R Foundation for Statistical Computing. http://www.R-project.org/.

Rosenberg, M. D., Zhang, S., Hsu, W. T., Scheinost, D., Finn, E. S., Shen, X., et al. (2016). Methylphenidate modulates functional network connectivity to enhance attention. *The Journal of Neuroscience, 36*(37), 9547–9557. doi:10.1523/JNEUROSCI.1746-16.2016.

Rubia, K., Halari, R., Cubillo, A., Mohammad, A. M., Brammer, M., & Taylor, E. (2009). Methylphenidate normalises activation and functional connectivity deficits in attention and motivation networks in medication-naive children with ADHD during a rewarded continuous performance task. *Neuropharmacology, 57*(7–8), 640–652. doi:10.1016/j.neuropharm.2009.08.013.

Rubia, K., Halari, R., Mohammad, A. M., Taylor, E., & Brammer, M. (2011). Methylphenidate normalizes frontocingulate underactivation during error processing in attention-deficit/hyperactivity disorder. *Biological Psychiatry, 70*(3), 255–262. doi:10.1016/j.biopsych.2011.04.018.

Sarter, M., Gehring, W. J., & Kozak, R. (2006). More attention must be paid: the neurobiology of attentional effort. *Brain Research Reviews, 51*(2), 145–160. doi:10.1016/j.brainresrev.2005.11.002.

Schubiner, H., & Katragadda, S. (2008). Overview of epidemiology, clinical features, genetics, neurobiology, and prognosis of adolescent attention-deficit/hyperactivity disorder. *Adolescent Medicine: State of the Art Reviews, 19*(2), 209–215 vii.

Sidlauskaite, J., Sonuga-Barke, E., Roeyers, H., & Wiersema, J. R. (2016). Altered intrinsic organisation of brain networks implicated in attentional processes in adult attention-deficit/hyperactivity disorder: a resting-state study of attention, default mode and salience network connectivity. *European Archives of Psychiatry and Clinical Neuroscience, 266*(4), 349–357. doi:10.1007/s00406-015-0630-0.

Silk, T. J., Malpas, C., Vance, A., & Bellgrove, M. A. (2016). The effect of single-dose methylphenidate on resting-state network functional connectivity in ADHD. *Brain Imaging and Behavior*. doi:10.1007/s11682-016-9620-8.

Silk, T. J., Vance, A., Rinehart, N., Bradshaw, J. L., & Cunnington, R. (2008). Dysfunction in the Fronto-parietal network in attention deficit hyperactivity disorder (ADHD): an fMRI study. *Brain Imaging and Behavior, 2*(2), 123–131. doi:10.1007/s11682-008-9021-8.

Silver, M., Montana, G., Nichols, T. E., & Alzheimer's Disease Neuroimaging, I. (2011). False positives in neuroimaging genetics using voxel-based morphometry data. *NeuroImage, 54*(2), 992–1000. doi:10.1016/j.neuroimage.2010.08.049.

Smith, S. M., Fox, P. T., Miller, K. L., Glahn, D. C., Fox, P. M., Mackay, C. E., et al. (2009). Correspondence of the brain's functional architecture during activation and rest. *Proceedings of the National Academy of Sciences of the United States of America, 106*(31), 13040–13045. doi:10.1073/pnas.0905267106.

So, Y., Noh, J., Kim, Y., Ko, S., & Koh, Y. (2002). The reliability and validity of Korean parent and teacher ADHD rating scale. *Journal of Korean Neuropsychiatric Association, 41*(2), 283–289.

Spinelli, S., Vasa, R. A., Joel, S., Nelson, T. E., Pekar, J. J., & Mostofsky, S. H. (2011). Variability in post-error behavioral adjustment is associated with functional abnormalities in the temporal cortex in children with ADHD. *Journal of Child Psychology and Psychiatry, 52*(7), 808–816. doi:10.1111/j.1469-7610.2010.02356.x.

Sripada, C. S., Kessler, D., & Angstadt, M. (2014). Lag in maturation of the brain's intrinsic functional architecture in attention-deficit/hyperactivity disorder. *Proceedings of the National Academy of Sciences of the United States of America, 111*(39), 14259–14264. doi:10.1073/pnas.1407787111.

Sripada, C. S., Kessler, D., Welsh, R., Angstadt, M., Liberzon, I., Phan, K. L., et al. (2013). Distributed effects of methylphenidate on the network structure of the resting brain: a connectomic pattern classification analysis. *NeuroImage, 81*, 213–221. doi:10.1016/j.neuroimage.2013.05.016.

Strobl, C., Malley, J., & Tutz, G. (2009). An introduction to recursive partitioning: rationale, application, and characteristics of classification and regression trees, bagging, and random forests. *Psychological Methods, 14*(4), 323–348. doi:10.1037/a0016973.

Subcommittee on Attention-Deficit/Hyperactivity, D, Steering Committee on Quality, I., Management, Wolraich, M., Brown, L., Brown, R. T., et al. (2011). ADHD: clinical practice guideline for the diagnosis, evaluation, and treatment of attention-deficit/hyperactivity disorder in children and adolescents. *Pediatrics, 128*(5), 1007–1022. doi:10.1542/peds.2011-2654.

Van der Oord, S., Prins, P. J., Oosterlaan, J., & Emmelkamp, P. M. (2008). Efficacy of methylphenidate, psychosocial treatments and their combination in school-aged children with ADHD: a meta-analysis. *Clinical Psychology Review, 28*(5), 783–800. doi:10.1016/j.cpr.2007.10.007.

Veer, I. M., Beckmann, C. F., van Tol, M. J., Ferrarini, L., Milles, J., Veltman, D. J., et al. (2010). Whole brain resting-state analysis reveals decreased functional connectivity in major depression. *Frontiers in Systems Neuroscience, 4,* doi:10.3389/fnsys.2010.00041.

Volkow, N. D., Fowler, J. S., Wang, G., Ding, Y., & Gatley, S. J. (2002). Mechanism of action of methylphenidate: insights from PET imaging studies. *Journal of Attention Disorders, 6*(Suppl 1), S31–S43.

Volkow, N. D., Wang, G. J., Fowler, J. S., Logan, J., Angrist, B., Hitzemann, R., et al. (1997). Effects of methylphenidate on regional brain glucose metabolism in humans: relationship to dopamine D2 receptors. *The American Journal of Psychiatry, 154*(1), 50–55. doi:10.1176/ajp.154.1.50.

Wang, J., Wang, X., Xia, M., Liao, X., Evans, A., & He, Y. (2015). GRETNA: a graph theoretical network analysis toolbox for imaging connectomics. *Frontiers in Human Neuroscience, 9*, 386. doi:10.3389/fnhum.2015.00386.

Wang, L., Zhu, C., He, Y., Zang, Y., Cao, Q., Zhang, H., et al. (2009). Altered small-world brain functional networks in children with attention-deficit/hyperactivity disorder. *Human Brain Mapping, 30*(2), 638–649. doi:10.1002/hbm.20530.

Watts, D. J., & Strogatz, S. H. (1998). Collective dynamics of 'small-world' networks. *Nature, 393*(6684), 440–442. doi:10.1038/30918.

Yang, Z., Kelly, C., Castellanos, F. X., Leon, T., Milham, M. P., & Adler, L. A. (2016). Neural correlates of symptom improvement following stimulant treatment in adults with attention-deficit/hyperactivity disorder. *Journal of Child and Adolescent Psychopharmacology, 26*(6), 527–536. doi:10.1089/cap.2015.0243.

Zang, Y. F., He, Y., Zhu, C. Z., Cao, Q. J., Sui, M. Q., Liang, M., et al. (2007). Altered baseline brain activity in children with ADHD revealed by resting-state functional MRI. *Brain Dev, 29*(2), 83–91. doi:10.1016/j.braindev.2006.07.002.

Zou, Q. H., Zhu, C. Z., Yang, Y., Zuo, X. N., Long, X. Y., Cao, Q. J., et al. (2008). An improved approach to detection of amplitude of low-frequency fluctuation (ALFF) for resting-state fMRI: fractional ALFF. *Journal of Neuroscience Methods, 172*(1), 137–141. doi:10.1016/j.jneumeth.2008.04.012.

Zuo, X. N., Xu, T., Jiang, L., Yang, Z., Cao, X. Y., He, Y., et al. (2013). Toward reliable characterization of functional homogeneity in the human brain: preprocessing, scan duration, imaging resolution and computational space. *NeuroImage, 65*, 374–386. doi:10.1016/j.neuroimage.2012.10.017.